

Vortex-Antivortex Pair Production in a First Order Phase Transition

Sanatan Digal, Supratim Sengupta and Ajit M. Srivastava *

Institute of Physics

Sachivalaya Marg, Bhubaneswar-751005, INDIA

We carry out numerical simulation of a first order phase transition in 2+1 dimensions by randomly nucleating bubbles, and study the formation of global U(1) vortices. Bubbles grow and coalesce and vortices are formed at junctions of bubbles via standard Kibble mechanism as well as due to a new mechanism, recently proposed by us, where defect-antidefect pairs are produced due to field oscillations. We make a comparative study of the contribution of both of these mechanisms for vortex production. We find that, for high nucleation rate of bubbles, vortex-antivortex pairs produced via the new mechanism have overlapping configurations, and annihilate quickly; so only those vortices survive till late which are produced via the Kibble mechanism. However, for low nucleation rates, bubble collisions are energetic enough to lead to many well separated vortex-antivortex pairs being produced via the new mechanism. For example, in a simulation involving nucleation of 20 bubbles, a total of 14 non-overlapping vortices and antivortices formed via this new mechanism of pair creation (6 of them being very well separated), as compared to 6 vortices and antivortices produced via the Kibble mechanism. Our results show the possibility that in extremely energetic bubble collisions, such as those in the inflationary models of the early Universe, this new mechanism may drastically affect the defect production scenario.

PACS numbers: 98.80.Cq, 11.27.+d, 67.57.Fg

1. Introduction

Production of topological defects has been a subject of great interest to condensed matter physicists, as well as to particle physicists in the context of the models of the early Universe [1]. Conventionally there have been two types of processes thought to be responsible for the production of defects. Pair production of defects-antidefects via thermal fluctuations [2] is one of them while the second process, usually known as the Kibble mechanism [3], arises from the formation of a domain structure after the phase transition. In the context of the early Universe, it is the Kibble mechanism which plays the dominant role as thermally produced defects are generally Boltzmann suppressed.

Recently, we have proposed a new mechanism for defect production which arises due to field oscillations [4]. This mechanism was first discussed by two of us in the context of systems with small explicit symmetry breaking terms [5], for the case when transition is of first order. There are many examples of such systems, such as axionic strings and Skyrmons for particle physics and liquid crystal defects in the presence of external fields for condensed matter systems. Subsequently, we showed that this mechanism is not limited to systems with explicit symmetry breaking. We analyzed the underlying physics

of the mechanism and showed that this mechanism is completely general [4]. It applies to the production of all sorts of topological defects and even for second order transitions involving quench from high temperatures.

With the demonstration of the general applicability of this mechanism, it becomes important to ask about its relative importance in determining the defect distribution arising in a phase transition. The numerical simulations (for the first order transition case) carried out in [4,5] considered certain *specific* field configurations of bubbles as the initial conditions and showed, in detail, how this new mechanism actually operates, and how much enhancement in vortex production may occur in certain favorable conditions. For example, for the explicit symmetry breaking case in [5] it was shown that in certain cases one may get up to ten vortices and antivortices produced from a single two bubble collision. Similarly, in [4] (for the case when no explicit symmetry breaking is present), it was shown that with certain favorable distribution of phases and bubble separation, vortex-antivortex pair may form via this mechanism which is as well separated as the ones which are typically produced via the Kibble mechanism.

However, as these initial conditions were specially chosen, it only shows the possibility that this mechanism *may* play an important role in phase transitions. What

*E-mail :
digal@iopb.ernet.in
supratim@iopb.ernet.in
ajit@iopb.ernet.in

one would like to know is the actual contribution of this mechanism for defect production in a phase transition where bubbles are randomly nucleated, because that is the only quantity which is of experimental interest. We address this problem in this paper and focus on the case of most general interest, when there is no explicit symmetry breaking involved. The case with the explicit symmetry breaking is very specialized and the dynamics of vortex production also very different from the case with no explicit symmetry breaking; even though the underlying mechanism is still the same, arising due to oscillations of the field. Explicit symmetry breaking leads to extra features in the dynamics which play a very crucial role in determining the defect abundance. For example, in presence of explicit symmetry breaking, the energetics of field oscillations in the coalesced portion of the bubbles is governed not only by the energy acquired by the bubble walls due to conversion of false vacuum to true vacuum, but also due to the energy stored in the bubble walls due to the tilt in effective potential. In order that such effects do not obscure the main point we are trying to study, which is to know the relative importance of this new mechanism in a general phase transition, we will only focus, in this paper, on systems with spontaneously broken global symmetry *without* any explicit symmetry breaking. In any case, it is these systems which form the most general class of systems where defect production is of interest, especially in the context of structure formation in the early Universe. We will present the study of defect production in phase transitions for the case of explicit symmetry breaking in a followup work [6].

The paper is organized in the following manner. The second section presents the essential physical picture of this mechanism by reviewing earlier results from [4]. Section 3 discusses the numerical technique used for implementing the phase transition by random nucleation of bubbles. We discuss the algorithm for detecting vortices produced in the transition. Each vortex is later analyzed in detail to make sure of its structure as well as the specific mechanism responsible for its production. We present this analysis and other numerical results in Section 4, where we identify vortices which are produced via the Kibble mechanism and those which are produced via the new mechanism. Section 5 provides discussion of the results where we compare vortex production via these two mechanisms and discuss various implications of the new mechanism. We argue that, due to this mechanism, in first order transitions with low nucleation rates (as would be the case for inflationary scenarios of the early Universe) violent bubble collisions may dramatically alter the production of defects. Conclusions are presented in Section 5 where we summarize the main features of our results.

2. Physical Picture of the Mechanism

As we mentioned above, the production of defect-

antidefect pairs via this mechanism happens entirely due to the oscillations of the magnitude of the order parameter field. We briefly review the essential physical picture underlying this mechanism, see [4]. We will study the formation of U(1) global vortices in 2+1 dimensions, with the order parameter being the vacuum expectation value of a complex scalar field Φ . Consider a region of space in which the phase θ of the order parameter field varies uniformly from α to β as shown in Fig.1a. At this stage there is no vortex or anti-vortex present in this region. Now suppose that the magnitude of the order parameter field undergoes oscillations, resulting in the passage of Φ through zero, in a small region in the center enclosed by the dotted loop, see Fig.1b. [As discussed in [4,5], and as we will see later in this paper, such oscillations can easily result during coalescence of bubbles in a first order phase transition. It can also happen in second order transitions involving quenching from high temperatures.] From a plot of the effective potential like that of a Mexican hat, it is easy to see that oscillation of the order parameter through zero magnitude amounts to a change in the order parameter to the diametrically opposite point on the vacuum manifold S^1 . This process, which causes a discontinuous change in θ by π , was termed as the flipping of Φ in [4].

For simplicity, we take θ to be uniform in the flipped region. Consider now the variation of θ along the closed path AOB CD (shown by the solid curve in Fig.1b) and assume that θ varies along the shortest path on the vacuum manifold S^1 (as indicated by the dotted arrows), as we cross the dotted curve i.e. the variation of θ from the unflipped to the flipped region follows the geodesic rule. [Even if θ varies along the longer path on S^1 , we still get a pair, with the locations of the vortex and the antivortex getting interchanged.] It is then easy to see that θ winds by 2π as we go around the closed path, showing that a vortex has formed inside the region. As the net winding surrounding the flipped region is zero, it follows that an anti-vortex has formed in the other half of the dotted region. One can also see it by explicitly checking for the (anti)winding of θ .

Another way to see how flipping of Φ results in the formation of a vortex-antivortex pair is as follows. Consider the variation of θ around the closed path AOB CD in Fig.1b before flipping of Φ in the dotted region. Such a variation of θ corresponds to a shrinkable loop on the vacuum manifold S^1 . After flipping of Φ in the dotted region, a portion in the center of the arc P connecting $\theta=\alpha$ to $\theta=\beta$ on S^1 moves to the opposite side of S^1 . If the midpoint of the arc originally corresponded to $\theta=\gamma$, flipping of Φ changes γ to $\gamma+\pi$. We assume that different points on the arc move to the opposite side of S^1 maintaining symmetry about the mid point of the arc, (and say, also maintaining the orientation of the arc). Then one can see that the loop on the vacuum manifold S^1 becomes non-shrinkable, and has winding number one, see [4] for details. Thus a vortex has formed inside the region enclosed by the solid curve. Obviously, an anti-

vortex will form in the left half of Fig.1b.

We should mention here that every successive passage of Φ through zero will create a new vortex-antivortex pair. Density waves generated during field oscillations lead to further separation of a vortex-antivortex pair created earlier. The attractive force between the vortex and anti-vortex lead to their eventual annihilation. Though, in a rapidly expanding early Universe, it is possible that the defect and antidefect may keep moving apart due to expansion. We emphasize that, as argued in [4], this mechanism is valid even for second order phase transitions, brought about by a quench from very high temperatures, and is also applicable for the formation of other topological defects. For example, it was shown in [4] that this mechanism also applies to the production of monopoles as well as textures. For string production in 3+1 dimensions, above arguments can easily be seen to lead to the production of string loops enclosing the oscillating region [4].

We mention here that there are vacuum manifolds for which the opposite orientations of the order parameter field are identified; for example liquid crystals with the vacuum manifold being RP^2 . In such cases, flipping of the order parameter field does not change its configuration, implying that this mechanism may not be applicable there under general situations. Though, it is possible to argue that in the presence of explicit symmetry breaking this mechanism should still be applicable, especially if the system is dissipative. This is because, for an order parameter configuration varying smoothly around the value which is energetically most unfavourable (due to explicit symmetry breaking), the only way to decrease the energy of the configuration is by creating a defect-antidefect pair as the field oscillates and passes through zero. We will discuss this in more detail in [6].

3. Numerical Techniques

The numerical techniques we use for bubble nucleation and time evolution are the same as used in [7]. In the following we provide essential aspects of the numerical method. We study the system described by the following Lagrangian in 2+1 dimensions.

$$L = \frac{1}{2}\partial_\mu\Phi\partial^\mu\Phi - \frac{1}{4}\phi^2(\phi - 1)^2 + \epsilon\phi^3 \quad (1)$$

This Lagrangian is expressed in terms of a dimensionless field Φ and appropriately scaled coordinates, with ϕ and θ being the magnitude and phase of the complex scalar field Φ . The theory described by this Lagrangian is that of a spontaneously broken global U(1) symmetry.

The effective potential in Eq.(1) has a local minimum at $\phi = 0$. The true minima occur at a non-zero value of ϕ and correspond to the spontaneously broken symmetry phase. At zero temperature, the phase transition takes place by nucleation of bubbles of true vacuum in the background of false vacuum (which is at $\phi=0$) via quan-

tum tunneling [8]. Bubbles nucleate with critical size and expand, ultimately filling up the space. The bubble profile ϕ is obtained by solving the Euclidean field equation [8]

$$\frac{d^2\phi}{dr^2} + \frac{2}{r}\frac{d\phi}{dr} - V'(\phi) = 0 \quad (2)$$

subject to the boundary conditions $\phi(\infty) = 0$ and $d\phi/dr = 0$ at $r = 0$; where $V(\phi)$ is the effective potential in Eq.(1) and r is the radial coordinate in the Euclidean space. In the Minkowski space, initial profile for the bubble is obtained by putting $t = 0$ in the solution of the above equation. θ takes a constant value inside a given bubble. Bubble nucleation is achieved by replacing a region of false vacuum by the bubble profile (which is suitably truncated while taking care of appropriate smoothness of the configuration). Subsequent evolution of the initial field configuration is governed by the following classical field equations in Minkowski space

$$\square\Phi_i = -\frac{\partial V(\Phi)}{\partial\Phi_i}, \quad i = 1, 2 \quad (3)$$

where $\Phi = \Phi_1 + i\Phi_2$. Time derivatives of fields are set equal to zero at $t = 0$.

To simulate a full first order transition we need to nucleate several such bubbles. This is done by randomly choosing the location of the center of each bubble with some specified probability per unit volume per unit time. Before nucleating a given bubble, it is checked if the relevant region is in false vacuum (i.e. it does not overlap with some other bubble already nucleated). In case there is an overlap then nucleation of the new bubble is skipped. Value of θ is randomly chosen for the interior of each bubble.

The simulation of the phase transition is carried out by nucleating bubbles on a square lattice with periodic boundary condition, i.e on a torus. The field configuration is evolved by using a discretized version of Eq.(3). Simulation is implemented by using a stabilized leapfrog algorithm of second order accuracy in both space and time. Physical size of the lattice taken is 320.0 x 320.0 with $\Delta x = 0.16i$ units. We choose $\Delta t = \Delta x/\sqrt{2}$ which satisfies the Courant stability criteria.

Simulations were carried out on a Silicon Graphics Indigo 2 workstation at the Institute of Physics, Bhubaneswar.

Bubbles are nucleated initially only, thus all the bubbles have same size as they expand. During the course of the phase transition, and in the *absence* of damping, the entire energy produced as a result of the conversion of false vacuum to true vacuum goes to increase the kinetic energy of the bubble walls. As a result, the bubble walls acquire a lot of energy which gets dissipated when bubbles collide. In bubble collisions (first studied in the context of the early Universe in [9]) there are two different modes, ϕ oscillation mode, and θ oscillation mode, in

which the energy stored in the bubble walls can be dissipated. The oscillations of ϕ (magnitude of Φ) produced, when two bubbles collide, depend on the θ difference as well as on the separation between the two bubbles. If the phase difference between the two bubbles is large, then most of the energy stored in the bubble walls is dissipated in smoothening out the phase gradient in the coalesced portion of the bubble walls and only a small amount of energy is converted to the ϕ oscillation mode. In the case of small phase difference between the two bubbles, a major portion of the energy of the bubble walls is converted to the oscillatory mode of ϕ . If the ϕ oscillations are sufficiently energetic then Φ may be able to climb the potential hill and overshoot the value $\Phi = 0$. Whenever this happens, a vortex-antivortex pair will be created, as we have discussed above. For a vortex-antivortex pair to be well formed and well separated, the value of ϕ should not be too close to zero in between the pair. This implies that Φ while passing through the value zero (which is the local minimum of $V(\phi)$) must be able to climb the potential hill in the same direction and roll down to the other side of $V(\phi)$. In the section that follows, we will be giving results of simulation to support this picture.

The location of the vortices was determined by using an algorithm to locate the winding number. As the phase transition nears completion via the coalescence of bubbles, magnitude of Φ becomes non-zero in most of the region with well defined phase θ . We divide each plaquette in terms of two (right angle) triangles and check, for each such triangle, whether a non-zero winding is enclosed. A non-zero winding is enclosed by the triangle if either of the following two conditions are satisfied. (1) $\theta_3 > \theta_1 + \pi$ and $\theta_3 < \theta_2 + \pi$; for $\theta_2 > \theta_1$, or (2) $\theta_3 < \theta_1 + \pi$ and $\theta_3 > \theta_2 + \pi$; for $\theta_2 < \theta_1$. Here, θ_1 , θ_2 , and θ_3 are the phases at the vertices of the triangle. Windings are detected only in regions where the magnitude of Φ is not too small in a small neighborhood of the triangle under consideration. If Φ is too close to zero in a region then that region is still mostly in the false vacuum and there is no stability for any windings present there. After getting *probable* locations of vortices using the above algorithm, we check each of these regions using detailed phase plots and surface plots of ϕ to check the winding of the vortex and to make sure that the vortex has well defined structure. By checking similar plots at earlier as well as later time steps we determine whether the vortex was produced due to oscillation, and subsequent flipping, of Φ , or via the Kibble mechanism.

In a recent work, Copeland and Saffine have studied two bubble collisions for the Abelian Higgs model [10]. It is shown in [10] that the geodesic rule in between the two bubbles is violated due to oscillations of ϕ , and vortex-antivortex pair is produced in that region. Here the gauge fields provide a driving force for θ leading to θ gradient in the coalesced region. More recently, they have also studied the formation of nontopological strings in bubble collisions [11]. In this context, we would like to emphasize that the only key ingredients for vortex-antivortex

pair creation via the new mechanism is a region of varying θ with large ϕ oscillation in the interior. [Thus, note that the variation of θ along a curve passing through the flipped region, e.g. along AOB in Fig.1b, also does not follow the geodesic rule.] Presence of other factors, such as gauge fields etc., can only affect the dynamical details of ϕ oscillations. For example, the dynamics of ϕ oscillations for the case with explicit symmetry breaking [5] is quite different from the case *without* explicit symmetry breaking [4], even though the underlying mechanism of vortex production is the same, i.e. via field oscillations.

4. Results of the Simulation

In this section we describe the results of a full simulation of the phase transition involving random nucleation of bubbles with low nucleation rate. We have also carried out simulations with large nucleation rates, these largely reproduce earlier results, as given in [7], where the extra vortex-antivortex pairs produced were highly overlapping and annihilated quickly. This happened because for large nucleation rates, average separation between bubble nucleation sites is small. Thus, bubble collisions were not energetic enough, due to low kinetic energies of the walls, to lead to sufficiently energetic field oscillations. In contrast, a low nucleation rate ensures that bubble collisions are very energetic. This leads to an increased possibility of flipping of Φ , thereby resulting in the creation of many well separated vortex-antivortex pairs, as we show below.

In the simulation, twenty bubbles are randomly nucleated with arbitrary phases chosen for bubble interiors. The bubbles expand and collide with each other, and vortices are formed at the junctions of three or more bubbles due to Kibble mechanism [3] as well as due to flipping of Φ in regions where field is oscillating. In our simulations we find a total (time integrated) of *seven well separated pairs*, i.e. 14 vortices and antivortices, forming due to the new mechanism of flipping of Φ . In comparison, we find that 6 vortices and antivortices are produced via the Kibble mechanism. Thus, for low nucleation rates, this new mechanism becomes very prominent, even for zero explicit symmetry breaking case. We count only those vortices which are separated by a distance which is *greater* than the core size of the string; the core size being of the order of the inverse of the Higgs mass ($\simeq 2.8$ for our case). Moreover, apart from these well separated pairs, there were many clusters of vortex-antivortex pairs which were highly overlapping. We have not counted these pairs as they annihilate quickly. The time for which a pair lasts depends upon many factors such as the presence of other vortices in the neighborhood, presence of field oscillations in the neighboring region which lead to density waves etc.

As we mentioned, we find a total of 6 vortices and antivortices which form via the Kibble mechanism. Formation of these vortices happens in a similar manner as was found in the simulations in [7]. However, the formation of vortex-antivortex pairs is now qualitatively differ-

ent. With the understanding of the precise mechanism underlying the formation of such pairs, we are now able to focus on simulations where formation of such pairs is the dominant process of defect creation. As we mentioned above, we achieve this by using a low nucleation rate for bubbles. Average separation between the bubble centers in the present case is about 65 units, which is about twice of the average separation used in [7]. [In the present simulation, bubble nucleation sites were restricted to be one radius away from the boundaries of the lattice, so that full bubbles are nucleated, bubble radius being about 13.8. In contrast, in [7], nucleation sites were restricted to be 5 bubble radii away from the lattice boundaries to avoid spurious reflections, due to use of free boundary conditions there.] As we will see below, the separation of vortices and antivortices in these pairs is now much larger, and these defects last for much longer times.

We now give some specific examples of vortex-antivortex pairs formed due to flipping of Φ . Fig.2 shows the plot of Φ for the entire lattice somewhat after the onset of phase transition. The bubbles have grown in size and some of them have collided. Fig.3a shows the Φ plot at $t = 49.8$ of a Kibble mechanism vortex located at $x = 62.8$, $y = 151.6$. The vortex is somewhat distorted and was formed by the collapse of a region of false vacuum, surrounded by true vacuum, with a net winding trapped in it. Such situations were also observed in [7] where the trapped false vacuum region was seen to assume spherical shape as it gradually collapsed. Due to the nature of formation of the vortex, the field near its core oscillates resulting in the flipping of Φ and subsequent formation of a vortex-antivortex pair due to flipping; as shown in Fig.3b at $t = 52.0$. The Kibble vortex is the right most one, at $x = 65.8$, $y = 151.0$, while the vortex and the antivortex created due to flipping are towards left of it, at $x = 58.6$, $y = 153.4$ and $x = 62.2$, $y = 149.8$, respectively. Note the flipped orientation of Φ in between this vortex and antivortex, compared to the orientation of Φ in the same region in Fig.3a. The vortex and the antivortex in this pair are well separated, by a distance equal to about 5, which is roughly twice the string core radius. Fig.3c shows the plot of Φ of the same region at $t = 54.3$. The anti-vortex belonging to the pair has moved closer to the Kibble mechanism vortex; (eventually annihilating it and leaving behind the *vortex belonging to the pair*).

There is another instance in which oscillations of the core of an antivortex formed via the Kibble mechanism give rise to a vortex-antivortex pair by the flipping mechanism. Here also, the Kibble antivortex forms due to the collapse of a region of false vacuum having net antiwinding. In this case, we find that the Kibble mechanism antivortex subsequently annihilates with the vortex belonging to the pair thereby leaving behind the *anti-vortex of the pair*. We consider the vortex/anti-vortex which survives to be effective Kibble mechanism vortex/antivortex and count it as such. These examples clearly show that the vortex and antivortex formed by this mechanism can

be separated far enough to mix with the Kibble mechanism vortices and hence affect the defect distribution formed via the Kibble mechanism.

In Figs.4a-4b we give another example of vortex-antivortex pairs forming due to flipping. Fig.4a gives the Φ plot in a region in which there is no net winding, though there are strong phase gradients. The plot of Φ of the same region at $t = 72.4$ shows a vortex-antivortex pair, Fig.4b. Comparison of the two plots clearly indicate that the vortex-antivortex pair is due to flipping. This is also confirmed by the surface plots of ϕ . The vortex-antivortex pair is well formed and reasonably well separated.

Figs.5a-5f show a series of plots depicting the formation (by the flipping mechanism) and evolution of two well separated vortex-antivortex pairs as well as a cluster of overlapping vortex-antivortex pairs. The vortex-antivortex pairs belonging to the cluster annihilate soon after formation. Fig.5a shows the Φ plot of the region, at $t = 67.9$, in which there is no net winding or antiwinding present but there are huge field oscillations (as confirmed by the surface plots). A triangular region of false vacuum is seen near the top left region together with two other oscillating regions. Fig.5b shows the plot of Φ of the same region at $t = 74.6$. Comparison with Fig.5a clearly shows that the thin strip of region seen in Fig.5a has flipped resulting in the formation of a vortex-antivortex pair. The vortex is at $x = 188.8$, $y = 156.7$, and has a well formed core while the antivortex is below it, towards left, and has a very large core where field is oscillating. The triangular region of false vacuum seen in Fig.5a has almost disappeared by now. [Oscillations brought about by collision of bubble walls leads to the formation of yet another vortex-antivortex pair due to flipping at $t = 70.1$. However, this pair is highly overlapping and annihilates soon. We therefore do not count it as a pair, since we are only interested in formation of those defects which can survive at least for a while, in order that they can affect the defect distribution. As we mentioned earlier, our criterion for counting a given vortex- antivortex pair is that the separation should be larger than the core thickness of the string.]

Fig.5c shows the same region at $t = 79.2$. Apart from the original pair, another pair is seen just below the vortex of the original pair, with the vortex and the antivortex of this second pair being separated along the x axis, with $y \simeq 153.8$. The core of anti-vortex, belonging to the original pair, has shrunk, though the anti-vortex is still distorted. Also, the formation of the new pair has led to further separation of the vortex and the antivortex belonging to the original pair, the separation being about 23 units at this stage. This is a very large separation, being almost an order of magnitude larger than the string core radius. Fig.5d shows the plot of Φ at $t = 81.5$. Both the pairs are now well-formed and well separated.

Subsequent Φ plot at $t = 86.0$ (Fig.5e) shows the vortex belonging to the newly formed pair moving to the anti-vortex belonging to the original pair (and ultimately

annihilating). The field oscillations generated by the annihilation of the pair leads to two new vortex-antivortex pairs (due to flipping) in the region. This is observed in the Φ plot of this region at $t = 90.5$. However, we do not count these pairs as they are not well separated and annihilate very soon. Fig.5f shows the plot of Φ of this region at $t = 90.5$, showing an isolated vortex and a region with net antiwinding. The vortex belonging to the original pair as well as the anti-vortex belonging to the pair formed at $t = 79.2$ do not annihilate till the end of the simulation, i.e. till $t = 101.8$. Of all the pairs formed due to flipping, this is the one which survives the longest.

5. Discussion of the Results

We have mentioned earlier that in order to have pair-production due to flipping of Φ , the bubble collisions must be sufficiently energetic. This is only possible for low nucleation rates for which bubble walls can acquire sufficient kinetic energy, before collision, by the conversion of false vacuum to true vacuum. Results obtained in [4] (the zero explicit symmetry breaking case), for a specific initial configuration, seemed to indicate that a pair production, where vortex and antivortex are well separated, may not occur too often. However, our results in this paper clearly indicate that even in a realistic phase transition where bubbles nucleate randomly, this new mechanism may become very prominent and may be the deciding factor in determining the defect distribution. In this context we mention that we find that the dynamics of collisions of several bubbles often conspires to enhance the magnitude of field oscillations thereby making flipping of Φ easier.

Another intriguing feature observed in our simulations is the presence of vortices/antivortices with an oscillating core. This feature is especially prominent in vortices/antivortices formed by the collapse of a large region of false vacuum in which a winding/anti-winding is trapped.

It is important to note that the results in [5] had shown that for systems with explicit symmetry breaking, this mechanism can produce very large number of defects. However, such systems are very special and in most cases (in condensed matter systems, or in particle physics, especially for models of structure formation in the early Universe) one is interested in defect production in systems *without* any explicit symmetry breaking. From this point of view, our present results are important as they demonstrate that for very low nucleation rates this mechanism may be most dominant for defect production. For example, this mechanism may completely dominate if one is interested in studying defect production at last stages of extended inflation in the early Universe [12] where bubble expansion is not impeded by damping. Cosmic string formation by Kibble mechanism has been studied in extended inflationary models in [13]. There it was argued that the correlation length, taken to be the mean bubble

size at the end of inflation, is larger than that corresponding to the Kibble mechanism for a thermal second order transition, and that this would result in the formation of a more dilute network of strings. In view of our results in this paper, one expects to see a fairly large number of small string loops in addition to the Kibble mechanism cosmic strings. [As we have mentioned, in three dimensions, the flipping of Φ will result in the formation of string loops [4].] This can drastically alter the number density of defects and may lead to a much denser network of strings.

For high nucleation rates and in the presence of damping, this mechanism will be considerably suppressed. This follows because the bubble walls will acquire less energy before collision thereby reducing the magnitude of Φ oscillations and the probability of flipping of Φ . In simulations with high nucleation rates, we find some highly overlapping pairs (as were found in [7]). Presence of these indicates that the magnitude of field oscillations is large enough to induce ϕ to pass through $\phi = 0$ thereby resulting in flipping, but *not* large enough to take ϕ all the way across the barrier to the other side of the effective potential which would result in the formation of a well separated pair.

The vortex-antivortex pairs eventually annihilate because of the attractive force between them. Even then, as we have shown above, in certain cases, density waves generated by field oscillations from neighboring regions, as well as the presence of other vortices lead to the separation of the pair, thereby delaying their eventual annihilation for a significant period of time. For three dimensions, this will imply formation of expanding string loops [4]. A dense network of such string loops can lead to formation of very long strings via intercommuting of entangled loops. In any case, a dense network of string loops will certainly modify the network of strings and hence can affect its subsequent evolution.

6. Conclusions

We have carried out numerical simulations of a general first order phase transition for the case of spontaneous breaking of a global U(1) symmetry, and have studied the production of vortices and antivortices. We estimate the net number of vortices produced, which includes vortices formed due to the Kibble mechanism as well as those produced via the pair production mechanism. Nucleation rate affects density of defects produced via the flipping mechanism due to the fact that a larger nucleation rate implies smaller average bubble separation, which in turn leads to less kinetic energy for the bubble walls before bubbles collide. Oscillations of ϕ are less prominent for less energetic walls leading to smaller number of defect-antidefect pairs for larger nucleation rates.

We therefore simulate the transition with a low nucleation rate. Here the bubble collisions are energetic enough to lead to large oscillations of ϕ and subsequent

flipping of Φ . This leads to the production of many, well separated, vortex-antivortex pairs via the new mechanism. For example, we find a total of 14, reasonably well separated, vortices and antivortices formed via this mechanism, as compared to 6 vortices and antivortices formed due to the Kibble mechanism. These results demonstrate that for very low nucleation rates, when bubble collisions are extremely energetic, this mechanism may drastically alter the defect production scenario. A dense network of defects produced via this mechanism can completely modify the network of strings produced via the Kibble mechanism and hence may alter the evolution of string network. This may be the situation for inflationary theories of the early Universe, for example, in extended inflation, where bubble collisions are very energetic. In fact in view of our results, one can expect a large population of other defects, especially monopoles, arising via this mechanism at the end of extended inflation.

Interestingly, a first order transition with low nucleation rate would imply large bubble separations and hence a smaller number of Kibble defects (say monopoles). However, defects (per bubble) produced via field oscillations are more abundant for low nucleation rate due to collisions being more energetic. Therefore, the final defect density may well be an increasing function of the bubble separation (say in extended inflation). In that case there seems a possibility of overproducing monopoles. This interesting possibility needs further exploration.

A direct experimental evidence for this mechanism can only come from condensed matter systems, as was the case for the Kibble mechanism [14]. The phase transition in superfluid ^3He from A to B phase is of first order, and occurs via nucleation of bubbles of true vacuum, the growth of which is unimpeded by damping. Hence, this mechanism should lead to formation of small string loops in this transition. In view of our results in this paper, we expect that number density of such string loops may be significant. It will be very exciting to detect these loops. As we had emphasized in [4], observation of loops smaller than the average size of coalescing bubbles, at the string formation stage, will give direct evidence for this mechanism.

- [6] S. Digal, S. Sengupta and A.M. Srivastava, (in preparation).
- [7] A.M. Srivastava, Phys. Rev. **D46**, 1353 (1992); see also, S. Chakravarty and A.M. Srivastava, Nucl. Phys. **B406**, 795 (1993).
- [8] M.B. Voloshin, I.Yu. Kobzarev and L.B. Okun, Yad. Fiz. **20**, 1229 (1974) [Sov. J. Nucl. Phys. **20**, 644 (1975)]; S. Coleman, Phys. Rev. **D15**, 2929 (1977); C.G. Callan and S. Coleman, *ibid.* **16**, 1762 (1977).
- [9] S.W. Hawking, I.G. Moss and J.M. Stewart, Phys. Rev. **D26**, 2681 (1982).
- [10] E.J. Copeland and P.M. Saffin Phys. Rev. **D15**, (1996).
- [11] E.J. Copeland and P.M. Saffin, hep-th/9702034.
- [12] D. La and P.J. Steinhardt, Phys. Rev. Lett. **62**, 376 (1989).
- [13] E.J. Copeland, E.W. Kolb and A.R. Liddle, Phys. Rev. **D42**, 2911 (1990).
- [14] For a review, see, W.H. Zurek, preprint, Los Alamos National Laboratory, LA-UR-95-2269 (July, 1996), cond-mat/9607135.

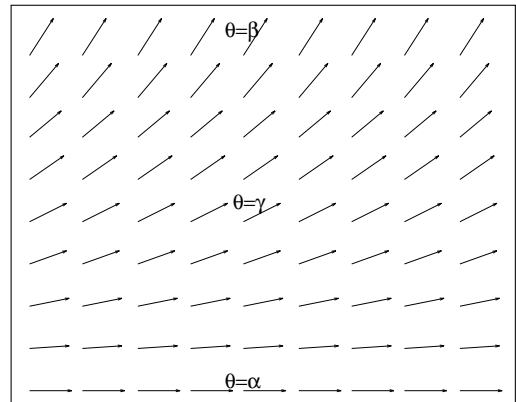


Fig.1a

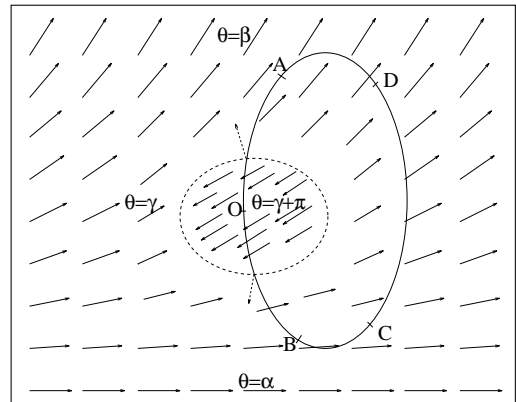


Fig.1b

-
- [1] For a review see, A. Vilenkin and E.P.S. Shellard, "Cosmic strings and other topological defects", (Cambridge University Press, Cambridge, 1994).
 - [2] F.A. Bais and S. Rudaz, Nucl. Phys. **B170**, 507 (1980).
 - [3] T.W.B. Kibble, J. Phys. **A9**, 1387 (1976).
 - [4] S. Digal, S. Sengupta and A.M. Srivastava, Phys. Rev. **D55**, 3824 (1997).
 - [5] S. Digal and A.M. Srivastava, Phys. Rev. Lett. **76**, 583 (1996).

FIG. 1. (a) A region of space with θ varying uniformly from α at the bottom to some value β at the top. (b) Flipping of Φ in the center (enclosed by the dotted loop) has changed $\theta = \gamma$ to $\theta = \gamma + \pi$ resulting in a pair production.

Field Plot At t = 67.9

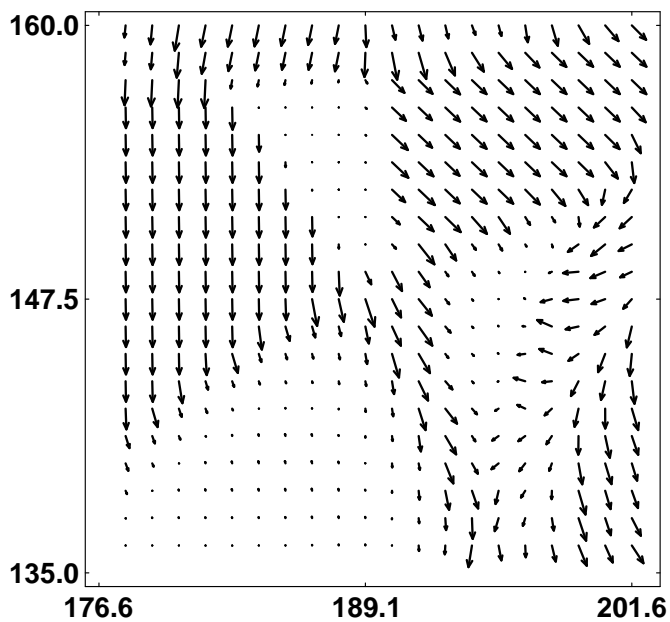


Fig.5a

Field Plot At t = 81.5

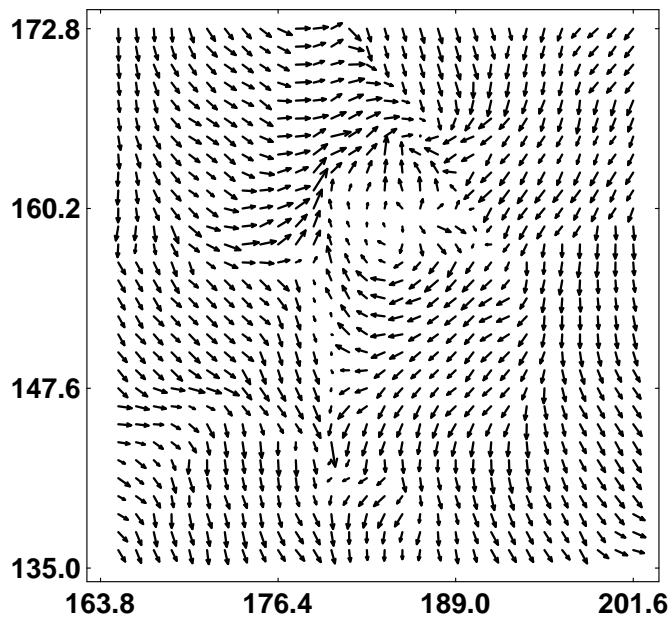


Fig.5d

This figure "fig1-1.png" is available in "png" format from:

<http://arxiv.org/ps/hep-ph/9705246v1>

This figure "fig1-2.png" is available in "png" format from:

<http://arxiv.org/ps/hep-ph/9705246v1>

This figure "fig1-3.png" is available in "png" format from:

<http://arxiv.org/ps/hep-ph/9705246v1>

This figure "fig1-4.png" is available in "png" format from:

<http://arxiv.org/ps/hep-ph/9705246v1>

This figure "fig1-5.png" is available in "png" format from:

<http://arxiv.org/ps/hep-ph/9705246v1>

This figure "fig1-6.png" is available in "png" format from:

<http://arxiv.org/ps/hep-ph/9705246v1>

This figure "fig1-7.png" is available in "png" format from:

<http://arxiv.org/ps/hep-ph/9705246v1>

This figure "fig1-8.png" is available in "png" format from:

<http://arxiv.org/ps/hep-ph/9705246v1>

This figure "fig1-9.png" is available in "png" format from:

<http://arxiv.org/ps/hep-ph/9705246v1>

This figure "fig1-10.png" is available in "png" format from:

<http://arxiv.org/ps/hep-ph/9705246v1>